(1990), p. 3] describes the San Andreas fault as a system of several major fault zones. Each comprises numerous fault segments consisting of individual faults. Geological segments are typically recognized by their geometry, but segments can be defined by their seismic rupture properties or by other geophysical characteristics common to contiguous faults of a fault zone. In (*11*) fault zones are defined in terms of contiguous straight fault segments, some of which were used in the present study. We did not consider segments smaller in length than the plate thickness (≈10 km), and we treated the Hayward, Calaveras, and San Gregorio faults as zones of groups of segments.

7. M. Lisowski, J. C. Savage, W. C. Prescott, *J. Geophys. Res.* **96**, 8369 (1991).
8. C. H. Scholz and P. A. Cowie, *Nature* **346**, 837 (1990); P. A. Cowie and C. H. Scholz, *J. Struct. Geol.*, in press.
9. C. H. Scholz, *The Mechanics of Earthquakes and Faulting* (Cambridge Univ. Press, Cambridge, 1991).
10. T. Rikitake, *Tectonophysics* **23**, 299 (1974).
11. R. Bilham and G. King, *J. Geophys. Res.* **94**, 10204 (1989); *U.S. Geol. Surv. Open-File Rep. 89-315* (1989), p. 80.
12. C. H. Jones and S. G. Wesnousky [*Science* **256**, 83 (1992)] and (*11*) quantify the effects of oblique slip near transpressional segments of the San Andreas fault system.
13. J. F. Pacheco, C. H. Scholz, L. R. Sykes, *Nature* **355**, 71 (1992); B. Romanowicz, *Geophys. Res. Lett.* **19**, 481 (1992).
14. G. C. P. King and J. Nabelek, *Science* **228**, 984 (1987); S. G. Wesnousky, *Bull. Seismol. Soc. Am.* **80**, 1374 (1990); R. H. Sibson, in *Earthquake Source Mechanics*, S. Das, J. Boatwright, C. H. Scholz, Eds. (Geophys. Monogr. 37, American Geophysical Union, Washington, DC, 1986), pp. 157–167.
15. It is common for displacements on strike-slip faults to exceed 10% of their total length (*8, 9*); S. G. Wesnousky, *Nature* **335**, 340 (1988); G. C. P. King, *Pure Appl. Geophys.* **124**, 567 (1986).
16. S. G. Wesnousky, *J. Geophys. Res.* **91**, 12,587 (1986).
17. A. J. Michael and D. Eberhart-Phillips, *Eos* **72**, 483 (1991).
18. In our model we used a transverse Mercator projection of the faults centered on the pole of rotation between the Pacific and North American plates [C. DeMets, R. G. Gordon, D. F. Argus, S. Stein, *Geophys. J. Int.* **101**, 425 (1990)].
19. S. L. Crouch and A. M. Starfield, *Boundary Element Methods in Solid Mechanics* (Allen and Unwin, London, 1989); our program was coded by G. C. P. King. Antisymmetric displacements applied to a single, vertical, frictionless fault, consisting of several contiguous elements in an elastic plate, resulted in a distribution of slip with a maximum near the center of the fault. The variation of slip along strike (in this case, elliptical in form) was evaluated numerically. The slip distribution on fault segments with complex fault geometries is discussed in (*11*). To obtain realistic slip distributions, we divided each fault zone into short straight segments (>10 km) consistent with the mapped geometry of each fault zone, and we divided each segment in the model into five or more contiguous subelements. More than 60 elements were used in some of the models.
20. D. J. Andrews, D. H. Oppenheimer, J. J. Lienkamper, *J. Geophys. Res.*, in press.
21. Surface exposures of the active Maacama fault reveal that slip is distributed over several subparallel fault strands [E. H. Pampeyan, P. W. Harsh, J. M. Coakley, *U.S. Geol. Surv. Misc. Field Stud. Map 1217* (1981)]. Although fault creep at 2 mm/year was observed on one fault strand, a value for the total Holocene slip rate is unavailable [R. R. Upp, *Eng. Geol. (Amsterdam)* **27**, 375 (1989)]. The fault was outlined by microseismicity (*25*), and in (*16*) a value of 7 mm/year was adopted for seismic hazard estimates.
22. J. L. Lienkamper, *U.S. Geol. Surv. 1:24000 Map MF 2196* (1992); ———, G. Borchardt, M. Lisowski, *J. Geophys. Res.* **96**, 18,261 (1991).
23. T. M. Niemi and N. T. Hall, *Geology* **20**, 195 (1992).
24. J. S. Galehouse, *U.S. Geol. Surv. Open-File Rep. 91-352* (1991), p. 375.
25. W. L. Ellsworth, *U.S. Geol. Surv. Prof. Pap. 1515* (1990), p. 153; D. A. Castillo and W. L. Ellsworth *J. Geophys. Res.*, in press.
26. K. P. Furlong, W. D. Hugo, and G. Zandt [*J. Geophys. Res.* **94**, 3100 (1989)] have developed sophisticated three-dimensional rheological models for northern California based on its thermal history. Their application would be useful for improved models for examining fault connectivity in the region.
27. A. A. Barka and K. Kadinsky-Kade, *Tectonics* 7, 663 (1988).
28. The 80-km-long surface rupture of the Landers earthquake included several mapped and unmapped faults (Camp Rock, Johnson Valley, and Emerson faults) that were separated by more than 5 km.
29. K. E. Budding, D. P. Schwartz, D. H. Oppenheimer, *Geophys. Res. Lett.* **18**, 447 (1991).
30. S. F. McGill and K. E. Sieh, *J. Geophys. Res.* **96**, 21597 (1991).
31. E. Hauksson, in *Engineering Geology Practice in Southern California*, B. W. Pipkin and R. J. Proctor, Eds. (Association of Engineering Geologists Spec. Publ. No. 4, Southern California Section, Star Publishing, Belmont, CA, 1992), in press.
32. Supported by the NSF.

14 April 1992; accepted 13 July 1992

Mass-Spectrometric ^{230}Th-^{234}U-^{238}U Dating of the Devils Hole Calcite Vein

Kenneth R. Ludwig,* Kathleen R. Simmons, Barney J. Szabo, Isaac J. Winograd, Jurate M. Landwehr, Alan C. Riggs, Ray J. Hoffman

The Devils Hole calcite vein contains a long-term climatic record, but requires accurate chronologic control for its interpretation. Mass-spectrometric U-series ages for samples from core DH-11 yielded ^{230}Th ages with precisions ranging from less than 1,000 years (2σ) for samples younger than ~140 ka (thousands of years ago) to less than 50,000 years for the oldest samples (~566 ka). The $^{234}U/^{238}U$ ages could be determined to a precision of ~20,000 years for all ages. Calcite accumulated continuously from 566 ka until ~60 ka at an average rate of 0.7 millimeter per 10^3 years. The precise agreement between replicate analyses and the concordance of the $^{230}Th/^{238}U$ and $^{234}U/^{238}U$ ages for the oldest samples indicate that the DH-11 samples were closed systems and validate the dating technique in general.

Core DH-11 of the Devils Hole (DH) calcite vein contains a continuous record of stable-isotopic variation in Great Basin ground water for most of the past several hundred thousand years (*1*). Spectral analyses of ^{18}O and ^{13}C records of DH-11, as well as inferences on timing of glacial-interglacial transitions (*1*), rely on the accuracy of the chronometric control. To provide this control, we determined mass-spectrometric (MS) uranium-series ages (*3*) for 21 samples across DH-11, using replicate analyses to validate estimates of uncertainty.

For each analysis, ~300 mg of calcite chips were selected for visual purity and freedom from porosity. The chips were ultrasonically cleaned, dissolved in HNO_3, spiked with ^{229}Th, ^{233}U, and ^{236}U, and purified with conventional ion-exchange methods. The purified U and Th were loaded with colloidal graphite on separate Re filaments (*3*) and analyzed in an automated mass spectrometer (*4*). To evaluate both the precision and accuracy of the dates, we examined possible sources of bias and external variance in the measurements (*5*) using instrumental checks (*6*) and two levels of replicate analyses. Thus, we have not relied on precision estimates arising solely from the internal statistics of the mass-spectrometric analyses.

The primary standard for this study was a solution of Precambrian uraninite that has been shown to be in secular equilibrium (*7*). Analyses of spiked aliquots of this standard were performed after every few samples and provide a test of the reproducibility of single analyses. The mean single-analysis precision of $^{230}Th/^{238}U$ for the secular-equilibrium standard was 0.24% (2σ, 12 analyses, no apparent external variance) (*5*, *8*). For $^{234}U/^{235}U$, a proxy for $^{234}U/^{238}U$, the mean single-analysis precision was 0.31% (2σ, 29 analyses), including a resolvable external error of 0.25% (*5*, *9*). Therefore, an additional variance corresponding to the 0.25% external error was added to the internal variance for each $^{234}U/^{235}U$ analysis. The weighted-mean

K. R. Ludwig, K. R. Simmons, B. J. Szabo, A. C. Riggs, U.S. Geological Survey, Mail Stop 963, Federal Center, Denver, CO 80225.
I. J. Winograd and J. M. Landwehr, U.S. Geological Survey, National Center, Mail Stop 432, Reston, VA 22092.
R. J. Hoffman, U.S. Geological Survey, 705 Plaza Street, Carson City, NV 89701.
*To whom correspondence should be addressed.

$^{234}U/^{235}U$ ratio of the secular-equilibrium standard was 0.0075690 ± 0.0000045, which corresponds to a ^{234}U half-life of 245,290 ± 140 years (*10*). This value is in reasonable agreement with the half-life of 244,600 ± 700 years determined from AS (alpha spectrometric) measurements (*11*). For age calculations, we normalized our measured $^{234}U/^{235}U$ and $^{230}Th/^{235}U$ ratios for DH-11 samples relative to the corresponding ratios measured for the secular-equilibrium standard; this approach in effect results in $^{230}Th/^{238}U$ and $^{234}U/^{238}U$ activity ratios. Advantages of this procedure are that (i) systematic errors from spike miscalibration are eliminated, (ii) errors in calculated ages arising from uncertainties in the ^{234}U and ^{230}Th decay constants are demagnified, and (iii) systematic errors arising from uncorrected biases in MS measurement are largely canceled out.

In addition to replicate analyses of the secular-equilibrium standard, we evaluated the real precision of the analyses by replicating most DH-11 sample analyses, starting from a different set of calcite chips. Besides providing another check on the validity of the calculated errors for each analysis, the replicate analyses are also sensitive to small-scale, open-system histories of the samples. Replicate $^{234}U/^{238}U$ analyses agreed within analytical error at all sample ages. Replicate $^{230}Th/^{238}U$ analyses agreed within analytical error for samples that formed before 130 ka, but not for those that formed at ~60 and ~122 ka (Table 1 and Fig. 1). This excess error arises largely from the uncertainty in the locations of these samples (~0.7 mm) and the thicknesses of the sample bands (1 and 3 mm, respectively). Thus, for samples having analytical age uncertainties less than or comparable to the errors predicted from the uncertainty in sample locations (that is, samples younger than ~200 ka), the actual scatter of replicate $^{230}Th/^{238}U$ ratios is expected to be somewhat greater than analytical error. These concerns are taken into

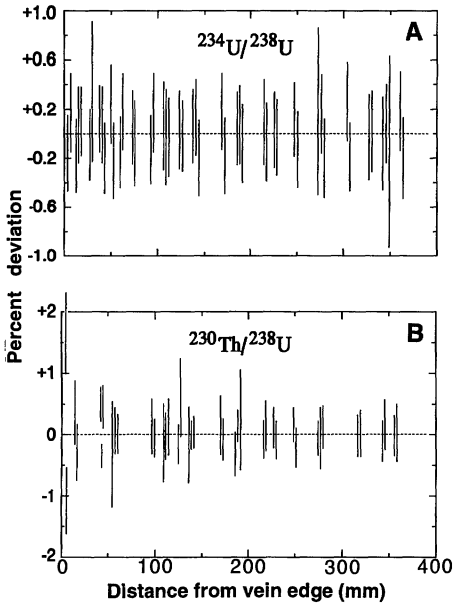

Fig. 1. Agreement between measured isotopic ratios for replicate DH-11 sample analyses. The *y*-axis indicates deviation, in percent, from weighted-mean value for each sample location. Height of vertical lines indicates 2σ analytical error for each replicate analysis (sample locations for each group of replicates expanded in *x*-direction for clarity: each clump of vertical lines represents replicate analyses for one sample location). Excess scatter of $^{230}Th/^{238}U$ age replicates of the youngest samples probably arises from non-reproducibility of sample locations (see text).

Table 1. Mass-spectrometric U-series ages (thousands of years) and calculated initial $^{234}U/^{238}U$ activity ratios of individual DH-11 samples versus distance from the free face of the vein (2σ errors). Calculated using half lives for ^{230}Th of 75,381 ± 590 and ^{234}U of 244,600 ± 490 years (2σ) (*11, 13*). Median U content of the samples was 0.46 ppm (range = 0.30 to 0.58), median ^{232}Th was 0.33 ppb (range <.02 to 16). The ^{230}Th ages are almost unaffected by corrections for initial ^{230}Th, ^{234}U, and ^{238}U, although a small correction corresponding to an initial $^{232}Th/^{238}U$ atomic ratio of 3.8 ± 2.0 (^{230}Th, ^{234}U, and ^{238}U are assumed to be in secular equilibrium) was applied. ^{234}U ages of samples <385 ka are not shown (all agree with the corresponding ^{230}Th ages) because they are not truly independent ages. Uncertainties in ^{234}U ages arise almost entirely from the ±0.10 uncertainty in initial $^{234}U/^{238}U$ ratio (Fig. 4).

Distance (mm)	^{230}Th age	^{234}U age	Initial $^{234}U/^{238}U_{act}$	Observed $^{230}Th/^{232}Th_{act}$
Water			2.7693 ± 0.0066	
			2.7657 ± 0.0082	
1.0	61.5 ± 0.6		2.818 ± 0.010	104
	59.1 ± 0.5		2.816 ± 0.010	135
16.0	81.2 ± 0.7		2.787 ± 0.010	174
	80.2 ± 0.6		2.790 ± 0.010	215
	80.5 ± 0.5		2.792 ± 0.009	228
41.0	119.7 ± 1.0		2.666 ± 0.010	47,200
44.5	122.7 ± 0.8		2.656 ± 0.009	33,400
	121.1 ± 0.8		2.647 ± 0.010	33,800
	123.3 ± 1.0		2.649 ± 0.010	36,700
48.5	131.9 ± 1.2		2.674 ± 0.011	1,370
54.0	149.7 ± 2.5		2.737 ± 0.016	8,280
	149.8 ± 1.4		2.749 ± 0.012	6,630
58.5	156.0 ± 1.2		2.769 ± 0.012	3,710
	156.4 ± 1.5		2.767 ± 0.014	4,100
98.5	212.5 ± 2.9		2.762 ± 0.018	4,370
	209.8 ± 2.4		2.759 ± 0.017	5,460
111.0	234.5 ± 4.9		2.748 ± 0.028	12,900
	235.9 ± 3.8		2.752 ± 0.024	9,730
	236.9 ± 3.9		2.757 ± 0.023	11,200
126.0	266.8 ± 4.2		2.797 ± 0.025	1,010
	274.0 ± 6.6		2.832 ± 0.036	766
137.0	283.3 ± 7.1		2.796 ± 0.038	3,140
	284.1 ± 4.2		2.803 ± 0.025	2,870
	288.6 ± 4.5		2.812 ± 0.026	2,300
171.5	326.1 ± 8.7		2.712 ± 0.044	2,270
	328.7 ± 7.5		2.710 ± 0.039	2,320
188.0	349.2 ± 8.9		2.782 ± 0.047	16,800
	356.9 ± 8.6		2.823 ± 0.046	16,100
	362 ± 18		2.844 ± 0.093	15,500
219.0	390 ± 13	385 ± 20	2.774 ± 0.068	65,400
	401 ± 15	386 ± 20	2.821 ± 0.079	64,600
227.0	404 ± 14	411 ± 20	2.716 ± 0.069	31,300
	400 ± 13	411 ± 20	2.895 ± 0.064	35,000
250.0	439 ± 17	435 ± 20	2.773 ± 0.087	33,500
	437 ± 18	437 ± 20	2.749 ± 0.091	36,400
277.0	473 ± 43	459 ± 22	2.82 ± 0.23	71,200
	474 ± 31	459 ± 20	2.82 ± 0.16	98,300
	509 ± 34	463 ± 21	2.99 ± 0.19	76,700
318.5	507 ± 35	510 ± 20	2.74 ± 0.17	11,100
	555 ± 49	515 ± 20	2.96 ± 0.27	3,250
334.5	535 ± 44	532 ± 21	2.77 ± 0.22	294
	531 ± 47	531 ± 21	2.75 ± 0.23	415
344.5	584 ± 71	547 ± 21	2.94 ± 0.39	73,800
		545 ± 20		
	637 ± 192	548 ± 24	3.2 ± 1.2	63,400
357.5	560 ± 53	563 ± 21	2.73 ± 0.26	3,330
	630 ± 109	568 ± 21	3.09 ± 0.65	710

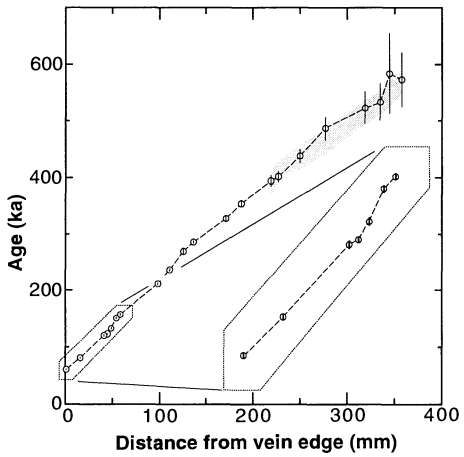

Fig. 2. Ages of DH-11 samples (weighted means of replicate analyses at each location; Table 2) versus distance from the free face of the core. Circles with vertical lines are ^{230}Th ages and 2σ uncertainties (including effect of nonreproducibility of sample locations; expanded in inset for youngest samples); shaded area represents ^{234}U ages (each at the same sample location as the ^{230}Th ages), and vertical dimension of shaded area indicates ^{234}U-age uncertainties.

Table 2. Weighted-mean ages (thousands of years) of DH-11 replicates (Table 1) versus distance from the free face of the vein. ^{230}Th ages are given for locations from 1.0 mm through 250.0 mm and ^{234}U ages are given for locations from 277.0 mm to 357.5 mm inclusive (because ^{234}U ages for these older samples are more precise). Weighting and error-propagation procedure considered uncertainties resulting from location errors (along the core) of each sample and also uncertainties from location errors of replicates within each sample. Thus the (2σ) errors in this table represent the total uncertainty of the ages at these locations within DH-11. Systematic errors arising from half-life uncertainties (*14*) and biases in the HU-1 secular-equilibrium standard (*15*) are small and are not included in age errors.

Distance (mm)	Weighted mean age
1.0	60.3 ± 1.7
16.0	80.6 ± 2.5
41.0	119.7 ± 2.1
44.5	122.4 ± 2.6
48.5	131.9 ± 3.0
54.0	149.8 ± 2.6
58.5	156.2 ± 3.1
98.5	211.0 ± 2.9
111.0	235.9 ± 3.1
126.0	269.1 ± 4.2
137.0	285.7 ± 3.5
171.5	327.5 ± 6.4
188.0	354.1 ± 6.2
219.0	395 ± 10
227.0	402 ± 10
250.0	438 ± 13
277.0	461 ± 20
318.5	513 ± 20
334.5	531 ± 20
344.5	546 ± 20
357.5	566 ± 20

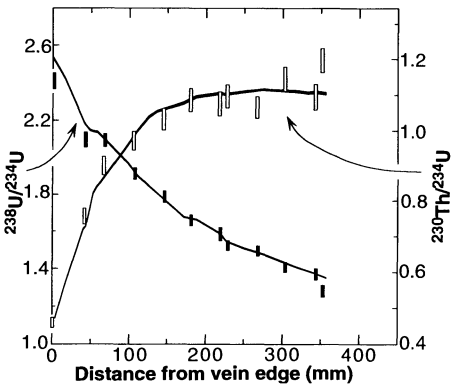

Fig. 3. Comparison of AS and weighted-mean MS analyses of DH-11. Jagged, heavy lines are MS analyses (line thickness defined by analytical uncertainties at each location); boxes are AS analyses (solid, ^{234}U/^{238}U activity ratios; open, ^{230}Th/^{234}U activity ratios; height of boxes indicates 2σ analytical uncertainty).

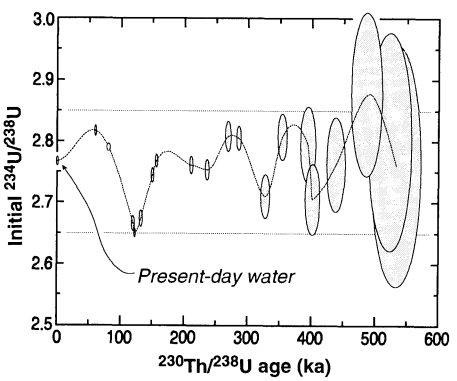

Fig. 4. Variation in weighted-mean initial ^{234}U/^{238}U activity ratios versus weighted-mean ^{230}Th ages of DH-11 samples (2σ uncertainties indicated by dimensions of ellipses). Horizontal dashed lines show approximate limits of variation of <350-ka samples, used to calculate uncertainties for ^{234}U ages of older samples.

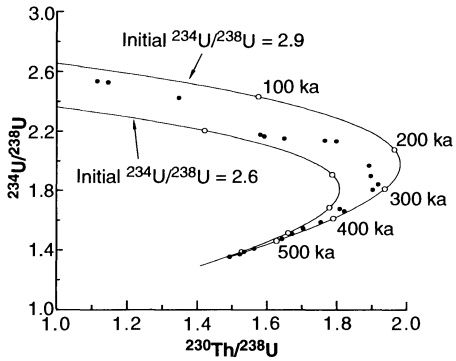

Fig. 5. ^{234}U-^{230}Th isotopic evolution of DH-11. Curved lines are closed-system isotopic evolution for initial ^{234}U/^{238}U activity ratios of 2.6 and 2.9. Open circles are ages on these evolution curves. Solid circles are activity ratios for DH-11 samples (weighted mean of replicate analyses except for youngest sample). Analytical errors are generally smaller than symbol size.

account in Table 2, wherein the data are weighted to account for both analytical and sample-location errors, in Figs. 2 to 4, and in assigning ages to the ^{18}O and ^{13}C time series (*1*).

The ^{230}Th ages for DH-11 increase monotonically and roughly linearly with distance in from the free face of the vein (Fig. 2 and Tables 1 and 2). All four of the samples having ^{230}Th ages >500 ka give meaningful ages (based on their consistency with the age-distance trend defined by the younger samples), and we thus conclude that even at an age of more than seven half-lives of ^{230}Th, the ages remain reliable. The AS analyses done on ~5-g samples from DH-11, although less precise than the MS analyses, are in essential agreement (Fig. 3) and validate the earlier AS dates on core DH-2 (*12*). Except for the cessation of vein growth at ~60,000 ka, the age-distance trend of DH-11 (Fig. 2) confirms the petrographic observations (*1*, *2*, *12*) that there were no detectable hiatuses in growth during the previous 500,000 years.

The AS analyses of 61,000- to 296,000-year-old samples from DH-2 (*12*) showed that, within the precision of the measurements, initial ^{234}U/^{238}U ratios that were back-calculated for these samples are indistinguishable from a mean value of about 2.70. Our analyses on DH-11 are consistent with this value, but, because of greater analytical precision, a secular variation in initial ^{234}U/^{238}U ratios can be readily resolved (Figs. 4 and 5). Weighted-mean initial ^{234}U/^{238}U ratios for the younger 360,000 years of DH-11 (where precision of the weighted-mean initial ratios is generally better than ±0.03) range from 2.651 ± 0.006 at 122.4 ka to 2.817 ± 0.007 at 60.3 ka. Uranium dissolved in present-day Devils Hole water has a ^{234}U/^{238}U activity ratio of 2.768 (weighted mean; Table 1), well within this range. Back-calculated initial ^{234}U/^{238}U activity ratios for the older DH-11 samples are necessarily less precise (because the ^{230}Th ages are less precise), but show no resolvable variation outside the limits defined by the younger samples. We calculated ^{234}U ages for DH-11 assuming that the average initial ^{234}U/^{238}U activity ratio was 2.75 ± 0.10 (Table 1 and Fig. 4). This value falls near the midpoint of the observed range, such that the uncertainty encompasses the extremes of the samples <360,000 years old. The age uncertainty (~20,000 years for all DH-11 samples) corresponding to this uncertainty in the initial ^{234}U/^{238}U ratio is much larger than the 2σ uncertainty arising from analytical error alone (2000 to 3000 years). Moreover, because the error arising from the uncertain initial ^{234}U/^{238}U ratio is likely to be highly correlated for closely spaced samples (the time constant for significant fluc-

tuations in initial $^{234}U/^{238}U$ ratio is probably thousands of years), we are unable to take advantage of replicate analyses to diminish the ^{234}U age uncertainties. Nonetheless, ^{234}U ages are more precise than the corresponding ^{230}Th ages for samples older than 450 ka and provide a useful check on the validity of the oldest ^{230}Th ages. The agreement between ^{234}U ages and ^{230}Th ages (Table 1) for the samples that formed >350 ka (and especially for those that formed >500 ka), independently confirms the ^{230}Th ages, and also shows that the growth rate of the vein for its first 100,000 years was similar to its long-term average growth rate.

Overall, the U-series ages form a remarkably self-consistent suite of age determinations. Because this consistency is both internal (from replicate samples) and external (from the stability of the overall age-distance trend), it seems highly unlikely that the dates have been significantly corrupted by open-system processes such as uranium gain or loss or alpha-recoil phenomena. The apparent ideality of the U-Th system in the vein material is probably the result of continuous submergence in water that showed limited secular variation of its physical and chemical properties (*2*).

REFERENCES AND NOTES

1. I. J. Winograd *et al.*, *Science* **258**, 255 (1992).
2. A. C. Riggs, in preparation.
3. J. H. Chen, R. L. Edwards, G. J. Wasserburg, *Earth Planet. Sci. Lett.* **80**, 241 (1986); R. L. Edwards, J. H. Chen, G. J. Wasserburg, *ibid.* **81**, 175 (1986).
4. Isotopic analyses were done with a VG-54E single-collector mass spectrometer using an analogue-mode Daly detector, controlled by the program ANALYST [K. R. Ludwig, *U.S. Geol. Surv. Open-File Rep. 85-141* (1985)]. U was analyzed in automatic mode with $^{235}U^+$ beams of $\sim 5 \times 10^{-14}$ A ($^{238}U/^{235}U$ ratio assumed to be 137.88); Th was typically analyzed with $^{230}Th^+$ beams of $\sim 10^{-15}$ A.
5. Internal variance is variance in isotopic ratios from within-run, MS measurement only. External variance is variance in isotopic ratios not accounted for by the internal variance.
6. Amplifier nonlinearity was calibrated by measurement of fractionation-corrected $^{235}U/^{238}U$ ratio over an ion-beam range of 5×10^{-16} to 4×10^{-13} A. A slightly nonlinear response of the Daly detector was detected, with ~0.3% less gain at 4×10^{-13} A than at 5×10^{-16} A. This (software-corrected) change in gain was approximately linear with beam size, and corrections were much less than measurement precision. A regression of $^{234}U/^{235}U$ ratio versus ion-beam intensity for hundreds of blocks of standard runs shows no resolvable residual nonlinearity. Mass fractionation during measurements was corrected by normalizing to measured $^{233}U/^{236}U$ ratios (from the 1:1 ^{233}U:^{236}U spike). No fractionation correction was applied to $^{230}Th/^{229}Th$ or $^{232}Th/^{229}Th$ ratios, because the average effect on $^{230}Th/^{229}Th$ was canceled out by the similarly uncorrected spike calibrations, and fractionation corrections on the $^{230}Th/^{232}Th$ ratio were unimportant. Each Re filament was doped with graphite before use, heated to running temperature in the mass spectrometer, and examined for mass-spectral purity. Isobaric interferences were absent during data acquisition, and blank levels of ^{230}Th were close to zero (average = $-0.8 \pm 4.0 \times 10^6$ atoms). Blanks for ^{238}U were negligible (median = 1.2×10^{-11} g), although blanks for ^{232}Th were significant (median = 4.6×10^{-12} g). Tails under the small peaks from nearby large peaks were insignificant (abundance sensitivity at 1 atomic mass unit offset was 2 to 4 ppm), as were amplifier time-constant effects.
7. Uraninite standard HU-1, obtained from M. Ivanovich, yielded U-Pb isotopic ages of 620 million years ago, concordant to within 0.5% (K. R. Ludwig, unpublished data). Alpha-spectrometric measurements yielded $^{234}U/^{238}U$ activity ratios of 0.9982 ± 0.0088 and $^{230}Th/^{234}U$ activity ratios within 0.5% of unity (J. N. Rosholt, personal communication to M. Ivanovich, 1979). The Precambrian age, concordance of U/Pb isotopic ages, and alpha-spectrometric measurements all indicate that the HU-1 standard is in, or very close to, secular equilibrium for $^{230}Th/^{238}U$ and $^{234}U/^{238}U$ ratios.
8. MSWD (mean square of weighted deviates) = 0.54.
9. MSWD = 2.0.
10. For a ^{238}U half-life of 4.4683×10^9 years [A. H. Jaffey, K. R. Flynn, L. E. Glendenin, W. C. Bentley, A. M. Essling, *Phys. Rev. C* **4**, 1889 (1971)].
11. P. de Bièvre *et al.*, in *Proceedings of the International Conference on Chemical and Nuclear Data, Measurement and Applications*, M. L. Hurrell, Ed. (Institute of Civil Engineers, London, 1971), pp. 221–225. Uncertainty given at 3σ level.
12. I. J. Winograd, B. J. Szabo, T. B. Coplen, A. C. Riggs, *Science* **242**, 1275 (1988).
13. J. W. Meadows, R. J. Armani, E. L. Callis, A. M. Essling, *Phys. Rev. C* **22**, 750 (1980).
14. For all samples, systematic age errors arising from uncertainty in the ^{230}Th half-life (*13*) are smaller than those from analytical errors (because of the error-demagnification effect of normalizing to the isotopic ratios of the secular-equilibrium standard). For those samples where ^{230}Th ages are preferred over ^{234}U ages, the worst-case age error from ^{230}Th decay-constant uncertainty is 1150 years (for the 235.9-ka samples at 111 mm), compared to the analytical error for that sample of 3100 years. Errors from ^{230}Th decay-constant uncertainties for all other samples <400 ka are less; errors for 400- to 600-ka samples rise exponentially from ~0 to 10 ka. Age errors arising from uncertainty in the ^{234}U half-life (*11*) are negligible for all samples.
15. For example, a 0.2% departure in the $^{230}Th/^{238}U$ ratio of the HU-1 standard from secular equilibrium would result in systematic ^{230}Th age errors that are negligible for the samples <300 ka, and about half the analytical error for the samples with ages from 327.5 to 438 ka.

16. Supported in part by the Climate Change Program of the U.S. Geological Survey.

22 April 1992; accepted 21 August 1992

Regulation of the Amount of Starch in Plant Tissues by ADP Glucose Pyrophosphorylase

David M. Stark, Kurt P. Timmerman,* Gerard F. Barry, Jack Preiss, Ganesh M. Kishore†

Starch, a major storage metabolite in plants, positively affects the agricultural yield of a number of crops. Its biosynthetic reactions use adenosine diphosphate glucose (ADPGlc) as a substrate; ADPGlc pyrophosphorylase, the enzyme involved in ADPGlc formation, is regulated by allosteric effectors. Evidence that this plastidial enzyme catalyzes a rate-limiting reaction in starch biosynthesis was derived by expression in plants of a gene that encodes a regulatory variant of this enzyme. Allosteric regulation was demonstrated to be the major physiological mechanism that controls starch biosynthesis. Thus, plant and bacterial systems for starch and glycogen biosynthesis are similar and distinct from yeast and mammalian systems, wherein glycogen synthase has been demonstrated to be the rate-limiting regulatory step.

The α-1,4 glucans (starch and glycogen) are the main storage carbohydrates in practically all living systems (*1*). In several crops, starch is a major component of the harvest and thus directly has an impact on yield. Within the last 10 years, the demand for starch has dramatically increased for both specialized food and industrial uses (*2*), primarily as a result of the development of high fructose corn syrups and bio-ethanol. A number of specialty starches (such as amylose and waxy starch) are being increasingly recognized for their superior material and nutritional properties as well as biodegradability. Understanding the critical components of the plant starch biosynthetic machinery therefore has a major impact on agriculture and industry. We have used transgenic plants to probe the rate-limiting step in starch biosynthesis.

Starch biosynthesis occurs in the plastids of plant cells, involving ADPGlc pyrophosphorylase (E.C. 2.7.7.27), starch synthase (E.C. 2.4.1.21), and branching enzyme (E.C. 2.4.1.18) (*1*, *3*). In view of its sensitivity to allosteric effectors, ADPGlc pyrophosphorylase (ADPGPP) has been suggested to play a pivotal role in plant starch biosynthesis, as it is in the bacterial pathway for glycogen biosynthesis.

The *Escherichia coli* ADPGPP, encoded by the *glg*C gene (*4*), is a regulated ho-

D. M. Stark, K. P. Timmerman, G. F. Barry, G. M. Kishore, Monsanto Company, 700 Chesterfield Village Parkway, St. Louis, MO 63198.
J. Preiss, Department of Biochemistry, Michigan State University, East Lansing, MI 48824.

*Present address: Pioneer Hi-Bred, 7300 Northwest 62 Avenue, Johnston, IA 50131.
†To whom correspondence should be addressed.